Caryologia
International Journal of Cytology, Cytosystematics and Cytogenetics

Firenze University Press
www.fupress.com/caryologia

OPEN ACCESS

Citation: A. Çetinbaş-Genç, F. Yanık, F. Vardar (2019) Histochemical and Biochemical Alterations in the Stigma of *Hibiscus syriacus* (Malvaceae) During Flower Development. *Caryologia* 72(4): 3-13. doi: 10.13128/cayologia-196

Published: December 23, 2019

Data Availability Statement: All relevant data are within the paper and its Supporting Information files.

Competing Interests: The Author(s) declare(s) no conflict of interest.

Histochemical and Biochemical Alterations in the Stigma of *Hibiscus syriacus* (Malvaceae) During Flower Development

Aslihan Çetinbaş-Genç*, Fatma Yanik, Filiz Vardar

Department of Biology, Marmara University, Istanbul, Turkey
*Corresponding author: aslihan.cetinbas@marmara.edu.tr

Abstract. The aim of this study is to determine the histochemical and biochemical changes that occurred during flower development in the stigmas of *Hibiscus syriacus*. The flower development of *H. syriacus* was divided into three successive stages; pre-anthesis, anthesis, post-anthesis, and stigma development was examined in parallel with these stages. At pre-anthesis, the stigmatic papillae cells covering the surface of the stigma were ovoid and their dense cytoplasm were rich in insoluble polysaccharide, protein and lipid. At anthesis, papillae cells grew and the pellicle layer becomes clear indicating dry-typed stigma. Meanwhile some sub-papillae cells, which accumulate dense organic matter from the beginning of development, began the process of autolysis and release their cellular content into the intercellular space. Whereas the organic matter content of papillae decreased at post-anthesis, it was still more than pre-anthesis stage. Similarly, peroxidase and non-specific esterase activity were very intensive at anthesis stage and activities were still remarkable at post-anthesis stage. The maximum CAT, SOD activity, H_2O_2 and MDA content were also determined at anthesis. Our results revealed that stigma of *H. syriacus* is receptive at anthesis and still conserve its receptivity at post anthesis assisting pollen germination and pollen tube growth.

Keywords. Anthesis, antioxidant enzyme, lipid peroxidation, papillae, stigma.

INTRODUCTION

Malvaceae family comprises 244 genera and more than 4225 species (Paoletti et al. 2009). Genus *Hibiscus* of Malvaceae has attracted considerable attention due to its large and attractive flowers. *Hibiscus syriacus* is the most popular species of this genus and has hermaphrodite flowers with white, pink, red, lavender, or purple color, depending on their cultivar (Punasiya and Pillai 2015). It consists of a tubular group of stamens surrounding the style which ends with the five branched stigma (Klips and Snow 1997; Çetinbaş-Genç and Ünal 2017).

Hibiscus syriacus has also a great social and economic importance whose flowers and seeds are frequently used in industry. It is mainly used in pharmaceutical products for the treatment of cardiovascular, urinary tract, skin,

and reproductive system diseases. Besides, it is often used in the production of hair-skin care products, perfumes, and used as a natural colorant in the beverage industry, and a source of fiber in the paper industry (Hsu et al. 2015).

To gain knowledge about the plant reproductive biology concerning pollination and fertilization helps to improve reproductive success which has direct effect on yield quality and economic benefits. Pollination involves a complex set of cell-cell communications that enable pollen-pistil interaction. This molecular interaction between the pollen wall and components of the stigmatic surface determines whether fertilization will take place (McInnis et al. 2006). Besides, stigma receptivity is one of the essential events for the start of pollen-pistil interaction. In many angiosperms, the stigma is receptive during anthesis but in some cases, the stigma may be still receptive after or even before anthesis (Brito et al. 2015). Therefore, the developmental characteristics of stigma are the focal point for pollination biology studies.

Despite their morphological diversity, the stigma of angiosperms is divided into two main groups: wet and dry typed. Although wet stigmas produce large surface secretions, dry stigmas are lack of secretions and its cuticle is coated with a proteinaceous surface layer. Despite these fundamental differences between wet and dry stigmas, high level of enzymatic activities indicates that stigmatic enzymes are essential for stigma function in both stigmatic types (Souza et al. 2016). Stigma includes heterogeneous components such as proteins, lipids, carbohydrates, amino acids and phenolic acids playing an important role in the pollen germination and tube growth on the stigma surface. These compounds present as a content of the exudate in wet stigmas, but in dry type stigmas they take place as a dry extracellular layer on the cuticle (Edlund et al. 2004).

The receptive surface of stigma is also characterized by the expression of biomolecules such as the peroxidases, esterases and reactive oxygen species (McInnis et al. 2006). It has been revealed that stigma shows high peroxidase and esterase activity in many plants when it gains receptivity for pollination (Hiscock et al. 2002). Besides, peroxidases and non-specific esterases are functional on the pollen-stigma interaction to loosen cell wall components of stigma cells with the aim of allowing pollen tubes to penetrate, and grow into the stigma (Hiscock et al. 2002; McInnis et al. 2006). Peroxidases generally catalyze the reduction of a wide range of organic substrates using hydrogen peroxide (H_2O_2) (McInnis et al. 2006). Stigmatic peroxidases and indirectly H_2O_2 metabolism form the components of signaling systems that mediate the identification of the proper pollens during pollen-stigma interaction (Cheong et al. 2002; Delannoy et al. 2003; Do et al. 2003).

In many cellular processes including development and tolerance to environmental stress, reactive oxygen species (ROS) also play a role as secondary messengers at low concentrations (Yanık et al. 2018). However, high concentrations of ROS cause harmful chain effects in the cell. Detoxification of ROS is carried out with antioxidant enzymes and non-enzymatic antioxidant systems. Superoxide dismutase, catalase, and peroxidase are some of the important antioxidant enzymes involved in the detoxification of ROS (Yanık et al. 2018). ROS have a role in signaling networks promoting pollen germination and pollen tube growth on stigma (McInnis et al. 2006; Hiscock and Allen 2008; Zafra et al. 2010). The concentration of ROS on the stigma affects the stigma receptivity, pollen germination and as a result the success of pollination. Therefore, in order to understand the pollination biology in detail, it is very important to examine the balance between production and detoxification of ROS during the development of the stigma.

The aim of the current study is to evaluate the histochemical and biochemical alterations of stigma in *H. syriacus* during the defined flowering stages; pre-anthesis (the period before anthesis), anthesis (the period in which flower is fully open and functional), and post-anthesis (the period after anthesis). Knowledge on stigmatic development will improve our information about the pollination success in plants as well as in *Hibiscus* varieties which have agronomic and ornamental potential.

MATERIAL AND METHODS

Flowers of *Hibiscus syriacus* L. were collected in June-August (2016-2018) in the vicinity of Göztepe-İstanbul (Turkey). Pistils at the different developmental stages were determined by stereomicroscope EZ4HD (Leica, Germany) and photographed by LAS EZ software.

Pistils were removed from flowers and fixed overnight in 3% (w/v) paraformaldehyde in 0.05 M sodium cacodylate buffer (pH 7.4) at 4 °C. After dehydration process with ethanol series and embedded in Epoxy resin using propylene oxide. Semi-thin sections (1-2 μm) were stained with Periodic Acid-Schiff (PAS) (Feder and O'Brien 1968) for insoluble polysaccharides, with Coomassie Brilliant Blue (CBB) (Fisher et al. 1968) for proteins and, with Sudan Black B (SBB) for lipids (Pearse 1961).

The optical density of organic content in papillae and sub-papillary cells was measured at different developmental stages according to Rodrigo et al. (1997).

Images were converted to 8-bit gray-scale and the optical density was quantized from black-and-white images using the Image J software. The mean and standard deviation of 5 images captured over an area of 300 μm² for papillae and 100 μm² for sub-papillary cells were computed.

For determination of qualitative peroxidase activity, fresh stigmatic tissue was incubated in sodium-phosphate buffer (PBS- 0.1 M, pH 5.8) containing 15 mM guaiacol and 5 mM H_2O_2 for 60 min (Birecka et al. 1973). To establish qualitative non-specific esterase activity, fresh stigmatic tissue was incubated in incubation buffer containing 1 mM α–naphthol acetate, 0.06 M Na_2PO_4, 0.01 M $NaNO_2$ and 2 M pararosaniline chloride for 10 min at 37 °C (Gomori 1950). After washing with dH_2O for 5 min, the stigmatic tissue squashed gently. All of the preparations were photographed with the KAMERAM software, assisted by a KAMERAM digital camera and an Olympus BX-51 microscope.

To evaluate the superoxide dismutase (SOD) and catalase (CAT) activity, 100 mg fresh stigmatic tissue were homogenized with 1 mL of cold PBS (50 mM, pH 7.0). After centrifugation at 14 000 rpm for 20 min at +4 °C, the supernatant was used as enzyme source. For CAT activity, 25 μL of the supernatant and 1 mL reaction mixture (20 mM PBS, pH 7.0 and 6 mM H_2O_2) were mixed and measured by the decrease in absorbance for 2 min at 240 nm, spectrophotometrically (Cho et al. 2000). For SOD activity, 2 μL of the supernatant and 2 mL reaction mixture (100 mM pH 7.0 PBS, 2 M Na_2CO_3, 0.5 M EDTA, 300 mM L-methionine, 7.5 mM nitro blue tetrazolium, 0.2 mM riboflavin) were mixed. After incubation under 15 W fluorescent lamps for 10 min, the mixture was measured at 560 nm, spectrophotometrically (Cakmak and Marschner 1992).

To measure the amount of hydrogen peroxide (H_2O_2) 300 mg fresh stigmatic tissue were homogenized with 2 mL extraction buffer (0.1% TCA, 1 M KI, 10 mM PBS) and centrifuged at 12 000 g for 15 min at 4 °C. After incubation in dark for 20 min, the supernatants were measured at 390 nm, spectrophotometrically (Junglee et al. 2014).

Lipid peroxidation (LPO) was determined by the production of malondialdehyde (MDA) level. 200 mg fresh stigmatic tissue were homogenized with 1 mL 0.1% TCA and centrifuged at 12 000 g for 20 min at +4 °C. 250 μL supernatant and 1 mL reaction mixture (0.6% TBA in 20% TCA) were mixed and incubated for 30 min at 95 °C. After cooling on ice, the mixture was centrifuged at 12 000 g for 10 min and the supernatant was measured at 532 and 600 nm, spectrophotometrically (Cakmak and Horst 1991).

All measurements and quantifications were repeated at least 3 times. Statistical analysis was performed using one-way analysis of variance (ANOVA), (SPSS 16.0 software). The significance of the applications was designated at the $P < 0.05$ level using the Tukey's test. All data presented are means ± SD.

RESULTS

In the current study, the stigma of *Hibiscus syriacus* analyzed in three successive stages (pre-anthesis, anthesis, and post-anthesis) correlated with some morphological markers such as color, the position of calyx and corolla, anther dehiscence, and the absence or presence of pollen on it.

In the stage of pre-anthesis, the flower buds of *H. syriacus* were ovoid with calyx covering half of the bud. Five stigmatic branches were very close to each other. There were no pollen grains on the stigma, because the anthers were still indehiscent (Figure 1 a,d,g). At anthesis stage, the flower was fully opened and their petals elongated. Stigma presented five distinctly separated branches with yellowish color. A lot of pollen grains were visible on the stigma due to anther dehiscence (Figure 1 b,e,h). At post-anthesis stage, the color of the petals began to fade and turned to brown, however a lot of pollen grains were still deposited on the stigma surface (Figure 1 c,f,i).

Hibiscus syriacus has capitate type stigma with five branches. The receptive surface of the stigma was covered with the tissue of unicellular papillae that are short, ovoid shaped, thin walled and tightly packed cells (Figure 2 a,f,k). Papillae cells lost their tight alignment with the increase of their width and length and their tips began to tape at anthesis. In the course of post-anthesis, papillae cells were much extended and thorn-shaped cells. At all stages of development, the dense cytoplasm of papillae cells was rich in insoluble polysaccharide, protein and lipids (Figure 2, Figure 3). The pellicle layer which was not very distinct at pre-anthesis became evident at anthesis (Figure 2 f). The papillae surfaces were covered with continuous pellicle and showed intense CBB staining indicating the dry-type stigma (Figure 2 g). The content of organic material in the papillae cells reached at maximum during anthesis (Figure 2 b,g,l). According to the optical density results, the insoluble polysaccharide content of papillae increased by 43 % (Figure 3 a), the protein content increased by 40 % (Figure 3 b), and lipid content increased by 77 % (Figure 3 c) at anthesis when compared to pre-anthesis. Besides, some of the sub-papillary cells accumulated a large

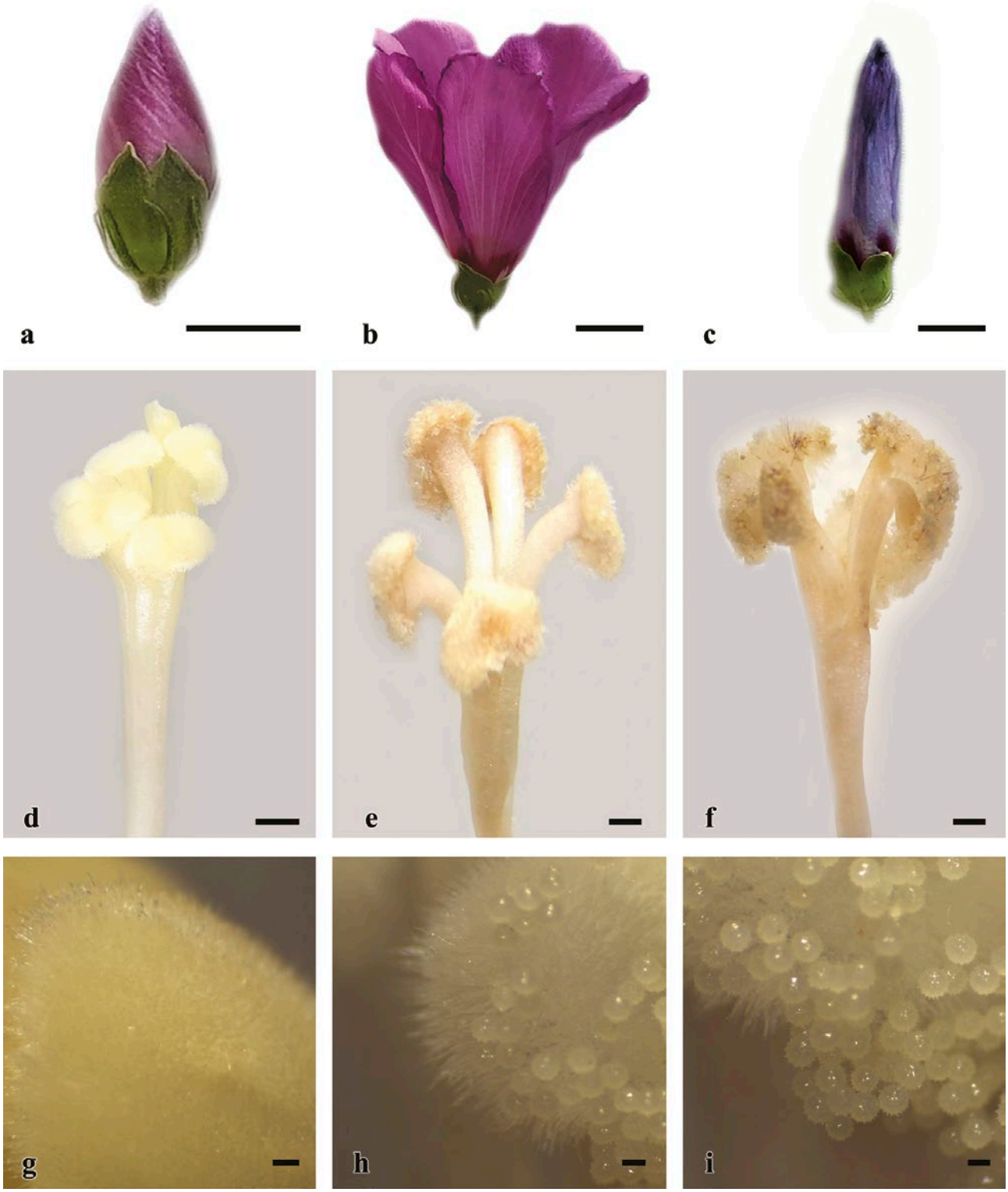

Figure 1. Determination of development stages of flower and stigma in *Hibiscus syriacus*. Flower morphology at pre-anthesis (a), anthesis (b), post-anthesis (c). Stigma morphology at pre-anthesis (d), anthesis (e), post-anthesis (f). Stigmatic surface at pre-anthesis (g), anthesis (h), post-anthesis (i). Scale: 1 cm in a-c, 1 mm in d-f and 100 μm in g-i.

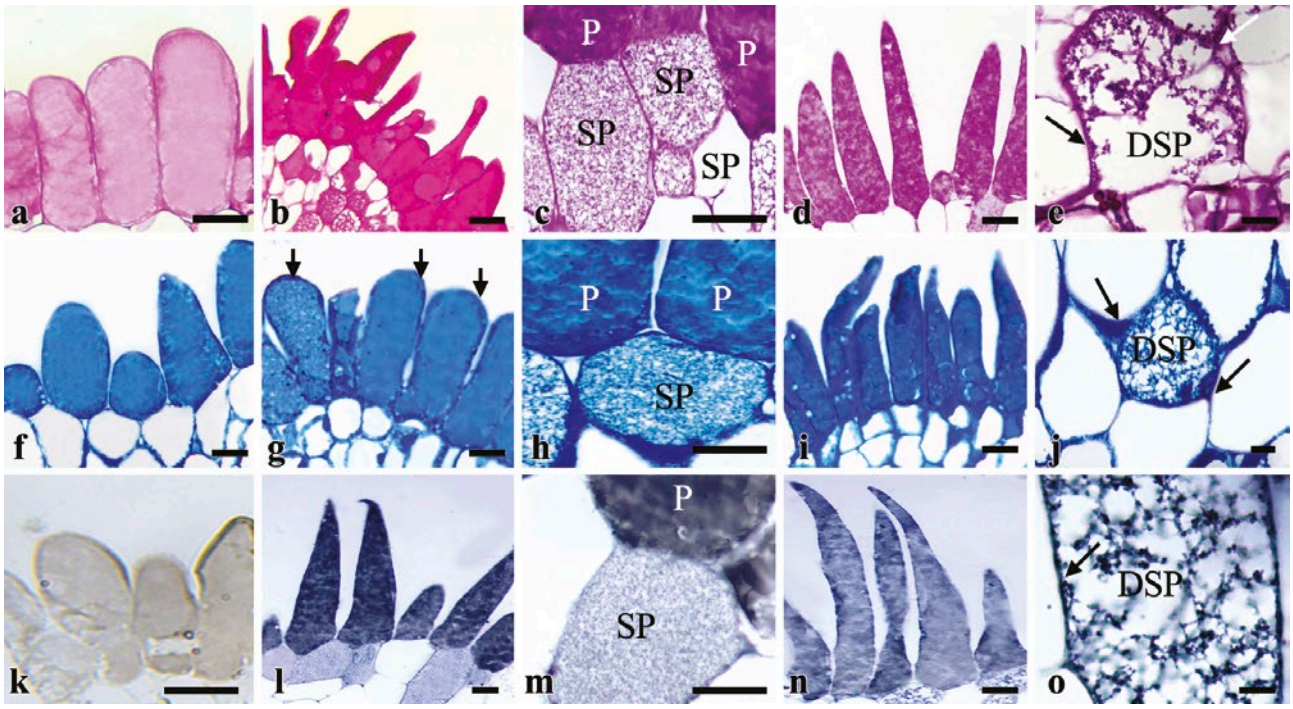

Figure 2. Semi-thin longitudinal sections of stigma of *Hibiscus syriacus* stained by PAS (a-e), CBB (f-j) and SBB (k-l). Short and ovoid papillae cells at anthesis (a, f, k). Papillae cells with dense organic material content and prominent pellicle layer (arrows) at anthesis (b, g, l). Sub-papillary cells that accumulate a large amount of organic material (c, h, m). Thorn shaped papillae with dense cytoplasm at post-anthesis (d, i, n). Degenerated subpapillary cells and their diffused contents to intercellular space (arrows) (e, j, o). P: Papillae cell, SP: Sub-papillary cell, DSP: Degenerated sub-papillary cell. Scale: 20 μm.

amount of organic matter during the transition from the pre-anthesis to anthesis. When sub-papillary cells started to degenerate at anthesis, their rich organic contents spread into the intercellular space indicating positive reaction with the PAS, CBB, and SBB staining (Figure 2 c,h,m)). At-post anthesis, the content of organic material papillae reduced in compare to anthesis (Figure 2 d,i,n)). The insoluble polysaccharide content of papillae was decreased by 10 % (Figure 3 a), the protein content was decreased by 18 % (Figure 3 b) and lipid content was decreased by 27 % (Figure 3 c) at post-anthesis with regard to anthesis. At this stage the pellicle got thinner (Figure 2 i). After the degeneration of sub-papillary cells, the accumulation of organic material at the intercellular space became more intense (Figure 2 e,j,o).

To measure the amount of starch granules in sub-papillary cells, the optical density of starch granules was measured after PAS staining. Although papillae cells had very few starch granules at all developmental stages, sub-papillary cells contained a large amount of dense starch granules representing a peak at anthesis (Figure 4 a-c). The starch content was increased by 109 % at anthesis (Figure 4 d) with regard to pre-anthesis. Despite the starch granule content decreased by 25 % at post-anthesis, it was still 55 % more than the pre-anthesis stage (Figure 4 c,d).

Based on our squash preparation results, non-specific esterase and peroxidase activity were not observed in stigmatic papillae cells at pre-anthesis (Figure 5 a,d). However, both enzyme activities gave progressive positive reaction at anthesis (Figure 5 b,e)). These positive activities indicated the stigma gains receptivity at this. Although the reduction of stigma receptivity at post-anthesis detected by poor reaction, it was still receptive in contrast to pre-anthesis (Figure 5 c,f)).

According to antioxidant enzyme activity results, the maximum CAT activity was determined at anthesis by 53 % while the minimum was observed at post-anthesis by 20 % in compare to pre-anthesis (Figure 5 g). Besides, the highest H_2O_2 production was observed at anthesis by 118 %, and lowest was observed at post anthesis by 6 % (Figure 5 h). Moreover, the SOD activity increased by 118 % at anthesis and 68 % at post-anthesis in compare to pre-anthesis (Figure 5 i). MDA one of the last products of lipid peroxidation was very high at anthesis and post-anthesis showing increase by 150 % and 116 %, respectively (Figure 5 j).

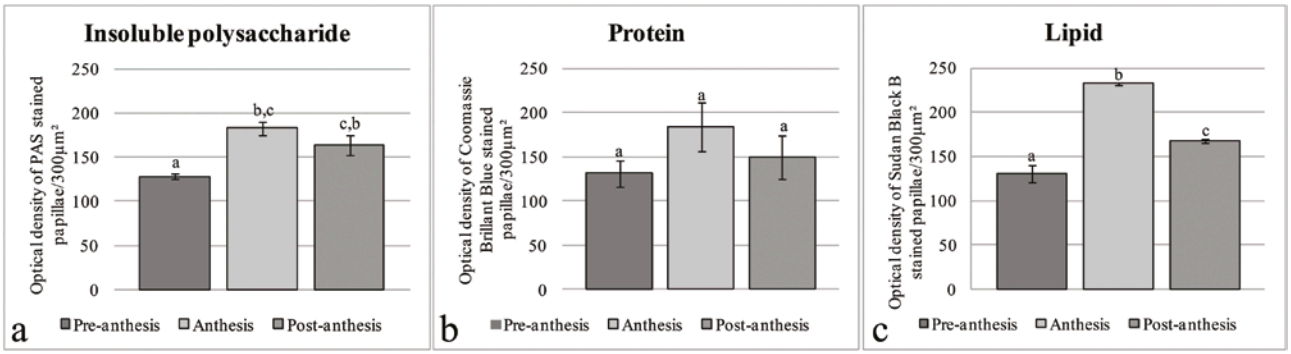

Figure 3. Organic material dynamics of papillae cells during stigma development of *Hibiscus syriacus*. a. Insoluble polysaccharide content, b. Protein content, c. Lipid content. Data are expressed as optical density per area unit (300 µm²). The data with different letters are significantly different according to Tukey's test at $P < 0.05$ for independent samples. Results are expressed as mean ± SD.

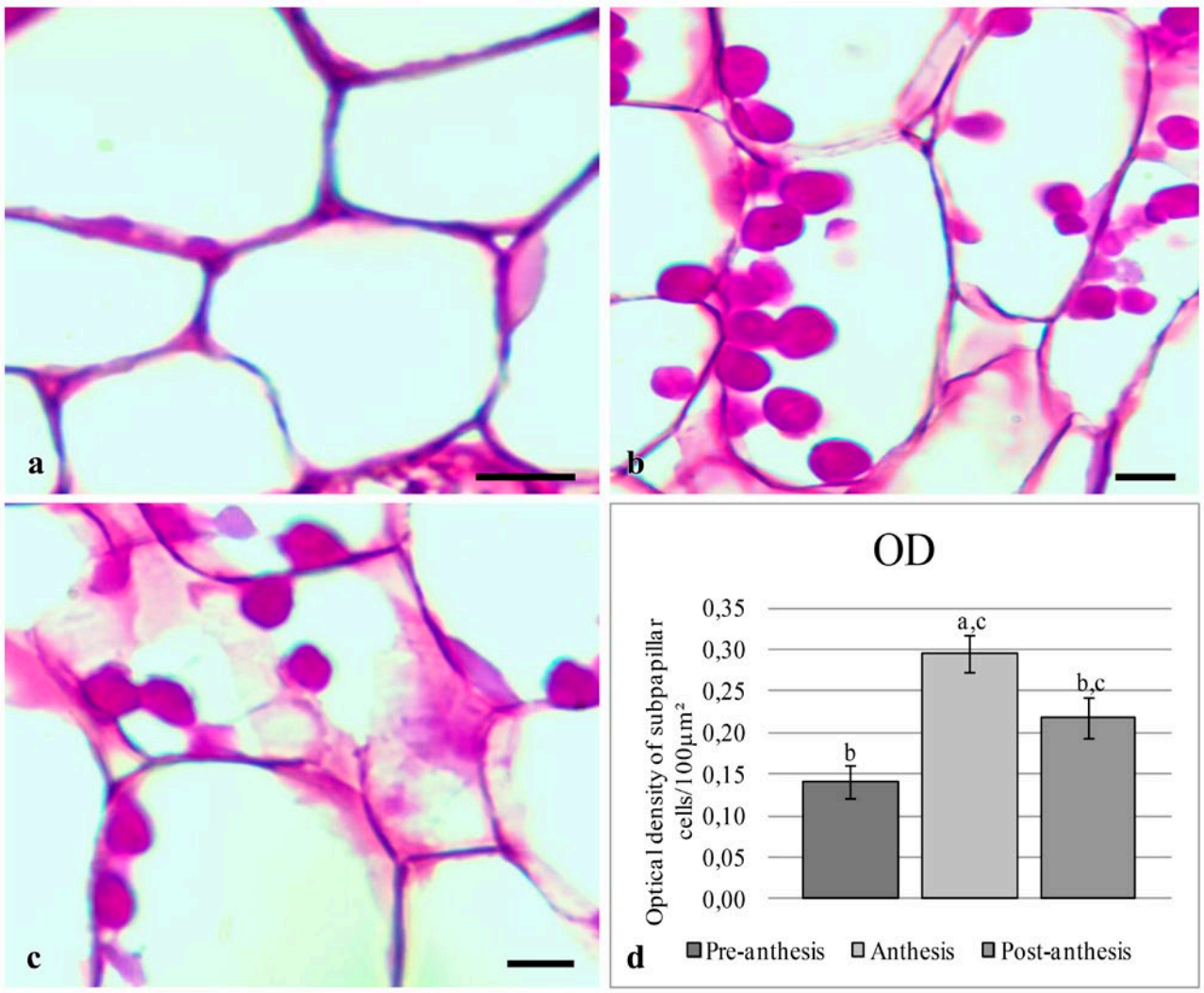

Figure 4. Starch dynamics at sub-papillary cells during stigma development of *Hibiscus syriacus*. a. Very few starch granules in sub-papillary cells at pre-anthesis, b. Large and dense starch granules in sub-papillary cells at anthesis, c. Starch granule content at post-anthesis (note the reduction in compare to anthesis), d. Starch synthesis/degradation pattern of sub-papillary cells, data are expressed as optical density per area unit (100 µm²). The data with different letters are significantly different according to Tukey's test at $P < 0.05$ for independent samples. Results are expressed as mean ± SD. Scale: 5 µm.

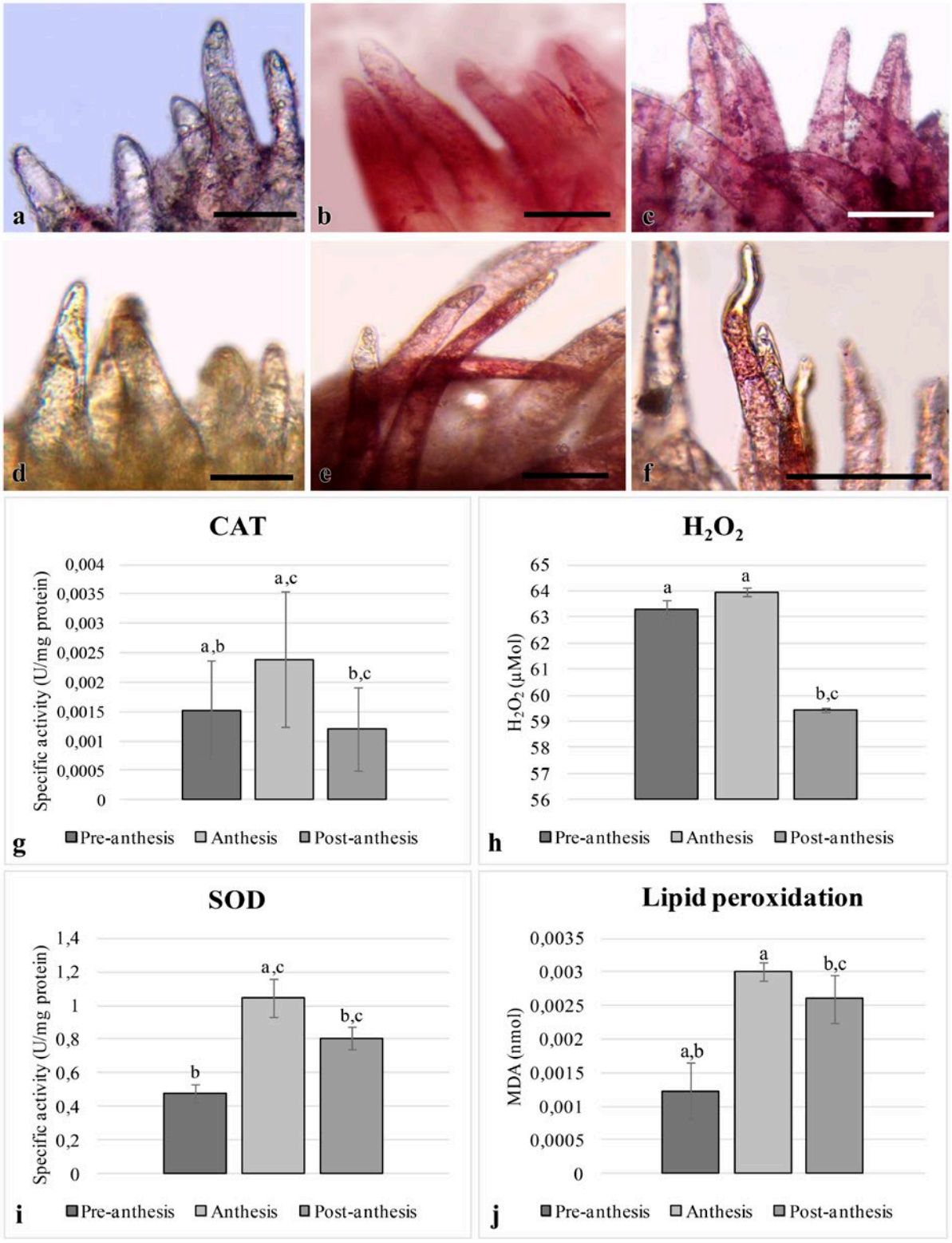

Figure 5. Enzymatic activities in stigma of *Hibiscus syriacus*. Non spesific esterase activity at pre-anthesis (a), anthesis (b), post-anthesis (c). Peroxidase activity at pre-anthesis (d), anthesis (e), post-anthesis (f), CAT activity (g), SOD activity (h), H_2O_2 content (i) and lipid peroxidation (j) of stigmas at different developmental stages. The data with different letters are significantly different according to Tukey's test at $P < 0.05$ for independent samples. Results are expressed as mean ± SD. Scale: 50 µm.

DISCUSSION

Flower development which is closely related to stigma differentiation may be categorized into different stages considering stigma (Suarez et al. 2012). Annahwi et al. (2017) previously defined the flower development stages of *Hibiscus rosa-sinensis* especially focusing on flower phenology. According to the researchers, we specified three stigma development stages in *Hibiscus syriacus* as a result of the examined morphological markers. *H. syriacus* and *H. rosa-sinensis* had similarities in flowering features. Calyx was longer than the corolla bud at pre-anthesis. Flowers were fully opened and anthers were dehiscent at anthesis. Annahwi et al. (2017) stated the last stage of flower development as fertilization, which was marked with the fall of the corolla, column, and pistil. But we preferred to name the last stage as post-anthesis, which was marked with shrinkage and discoloration of the corolla. The mature pistils of Malvaceae have been characterized as having five-branched and capitated stigma which was separated to each other during maturation in *H. syriacus* as it was in *H. rosa-sinensis* (Annahwi et al. 2017).

As a result of increased metabolic activity, it has been known that stigmatic papillae cells begin to accumulate polysaccharide, lipid, and protein throughout their development (Neil et al. 2002; Zafra et al. 2010). Lipids are reported to be effective in pollen hydration and growing pollen tube orientation. In addition, polysaccharides are known to form a suitable medium for pollen germination (Herrero and Dickinson 1979; Wolters-Arts et al. 1998). So, lipid and polysaccharides are found to be abundant on stigma, especially when it is ready for the pollination. Consistent with this, it was determined that stigmatic papillae cells of *H. syriacus* had an abundant polysaccharide, protein, and lipid content at all stages of development. However, their amounts were found to be at the maximum level at anthesis stage in which the stigma was the most receptive. Edlund et al. (2004) also stated that at the receptive stigma the formation of pellicle layer usually occurs. In *H. syriacus*, pellicle of papillae was formed at anthesis and it remained intact during the development. However, when stigma receptivity reduced at post-anthesis, the pellicle became thinner.

Degenerated sub-papillary cells were detected previously by Losada and Herrero (2012) in *Malus domestica* as it was in *H. syriacus*. The researcher stated that these cells contribute to the formation of stigmatic secretion. The release of their contents into the intercellular space provides the increment in the amount of secretion on the stigma surface and the intercellular space. Similar to *M. domestica*, organic material content in the intercellular space increased by degeneration of the sub-papillary cells in *H. syriacus*. However, there was no degeneration-based secretion on the stigmatic surface. Although degeneration-based organic material release started at post-anthesis, pellicle prevented the release of substances onto the stigma. According to the researchers the intercellular secretion has important roles in pollen recognition and germination (Heslop-Harrison 2000; McInnis et al. 2006). Besides, the accumulation of organic substances usually associated with stigma maturation and receptivity. It can be suggested that the accumulation of the substance in the intercellular space in *H. syriacus* was related to both maturity and receptivity at anthesis, however the continuation of the accumulation at post-anthesis may be associated with organ senescence rather than receptivity (Hiscock and Allen 2008).

Starch is principal storage carbohydrates having important roles on pollen tube growth, ovule and fruit formation and determination of flower quality in angiosperms (Chapin et al. 1990; Rodrigo et al. 2000; Reale et al. 2009; Alcaraz et al. 2010). Suarez et al. (2012) stated that the amount of starch increased in the sub-papillary cells and style channel during pollination in *Olea europaea*. In *H. syriacus*, whereas sub-papillary cells contained plenty of starch granules at pre-anthesis stage, along with pollination starch accumulation increased. At post-anthesis stage starch granules were still existed. Similarly, researchers noted that starches are reduced in stigmatic cells after pollination consuming as a source of energy for pollen tube growth (Rodriguez-Garcia et al. 2003).

Esterase and peroxidase are the major constituent of the stigma surface proteins. They are functional on the pollen-stigma interaction to loosen cell wall components of stigma cells with the aim of allowing pollen tubes to penetrate and grow into the stigma (Hiscock et al. 2002; McInnis et al. 2006). Their activity were determined on the surface of the receptive stigma in many species (Seymour and Blaylock 2000; Shakya and Bhatla 2010). In *H. syriacus*, the stigma exhibited poor non-specific esterase and peroxidase activity at pre-anthesis. But, intensive non-specific esterase and peroxidase activity detected at anthesis, indicating the stigma gained receptivity at this stage (Serrano and Olmedilla 2012). Although the expression of peroxidase decreased at post-anthesis with compare to the anthesis, it was more than pre-anthesis demonstrating that the stigma still continued to receptivity at post-anthesis. However, even in the case of a reduction in stigma receptivity, dense pollen grains, and continuing enzymatic activities represented that pollination still proceeds.

In recent years, many studies have reported that ROS function as signal molecules during the stigma - pollen interaction (McInnis et al. 2006; Zafra et al. 2010; Allen et al. 2011; Serrano and Olmedilla 2012). The most occurring ROS are superoxide anion ($O_2^{\cdot-}$), hydroxyl radical ($^{\cdot}OH$) and hydrogen peroxide (H_2O_2). Among them H_2O_2 which is produced by SOD from reduction of superoxide anions is the most stable ROS and it can cross the membranes. In angiosperm stigma, accumulation of H_2O_2 during the stigma receptivity is known to be a common feature. In parallel, H_2O_2 accumulation and SOD activity which is H_2O_2 catalyzer was at maximum level during the anthesis in *H. syriacus*. High concentrations of H_2O_2 may be involved in signaling networks that promote pollen germination and/or pollen tube growth on stigma as it was in *Arabidopsis thaliana* (McInnis et al. 2006). Furthermore, high levels of H_2O_2 can be produced as a result of increased metabolic activity in stigma papillae and surrounding tissues starting to collect pectin, arabinogalactan, proteins and other organic components, as well as starch and lipids (Neil et al. 2002; Zafra et al. 2010). It can be suggested that H_2O_2 concentration increased due to the accumulation of organic matter serving as a signal that promotes pollen germination and pollen tube entry at anthesis stage. It has been known that CAT breakdown H_2O_2 to H_2O and O_2 (Yanık et al. 2018). Although CAT activity increased at anthesis, H_2O_2 is still at high concentrations. This situation suggests that CAT activity is not sufficient to scavenge with over accumulated H_2O_2. ROS accumulation in papillae of *H. syriacus* indicates that stigma gains receptivity at anthesis. Supporting results were also stated in *Amygdalolia* and *O. europaea* cultivars (Aslmoshtaghi and Shahsavar 2016).

However, high concentrations of H_2O_2 cause oxidative stress resulting in biomolecular damage (Quan et al. 2008; Schieber and Chandel 2014). When the amount of ROS exceeds the threshold value, LPO occurs in both cell and organelle membranes and oxidative stress increases (Yanik et al. 2018). LPO can be monitored by the level of MDA that end product of LPO (Halliwell and Gutteridge 1989). Considering the highest H_2O_2 accumulation at anthesis, LPO was at highest level at anthesis in *H. syriacus* stigma. Furthermore, high MDA content may also relate to loosening of cell membrane components of papillae due to germinated pollen tubes at anthesis.

In conclusion, stigma of *H. syriacus* is receptive at anthesis stage and still receptive at post anthesis even its performance has fallen. At anthesis stage organic material synthesis, enzymatic activity, lipid peroxidation and H_2O_2 accumulation are very progressive assisting stigma receptivity, pollen germination and pollen tube growth. Our data will help improve our knowledge on pollination success in plants as well as in *Hibiscus*.

DISCLOSURE STATEMENT

No potential conflict of interest was reported by the authors.

REFERENCES

Alcaraz ML, Hormaza JI, Rodrigo J. 2010. Ovary starch reserves and pistil development in avocado (*Persea americana*). Physiol Plant. 140(4):395–404.

Allen AM, Thorogood CJ, Hegarty MJ, Lexer C, Hiscock SJ. 2011. Pollen–pistil interactions and self-incompatibility in the Asteraceae: new insights from studies of *Senecio Squalidus* (Oxford ragwort). Ann Bot. 108(4):687–698.

Annahwi D, Ratnawati R, Budiwati B. 2017. Flower and fruit development phenology and generative reproduction success of *Hibiscus rosa-sinensis* spp. YRU Journal of Science and Technology. 2(2):19–30.

Aslmoshtaghi E, Shahsavar AR. 2016. Biochemical changes involved in self-incompatibility in two cultivars of olive (*Olea europaea* L.) during flower development. J Hortic Sci Biotechnol. 91(2):189–195.

Birecka H, Briber KA, Catalfamo JL. 1973. Comparative studies on tobacco pith and sweet potato root isoperoxidases in relation to injury, indoleacetic acid, and ethylene effects. Plant Physiol. 52(1):43–49.

Brito MS, Bertolino LT, Cossalter V, Quiapim AC, Paoli HC, Goldman GH, Teixeira SP, Goldman MHS. 2015. Pollination triggers female gametophyte development in immature *Nicotiana tabacum* flowers. Front Plant Sci. 6:1–10.

Cakmak I, Horst JH. 1991. Effects of aluminum on lipid peroxidation, superoxide dismutase, catalase, and peroxidase activities in root tips of soybean (*Glycine max*). Physiol Plant. 83(3):463–468.

Cakmak I, Marschner H. 1992. Magnesium deficiency and high light intensity enhance activities of superoxide dismutase, ascorbate peroxidase, and glutathione reductase in bean leaves. Plant Physiol. 98(4):1222–1227.

Çetinbaş-Genç A, Ünal M. 2017. Timing of reproductive organs maturity in proterandrous *Malva sylvestris* L.. Not Sci Biol. 9(2):287–295.

Chapin III FS, Schulze ED, Mooney HA. 1990. The ecology and economics of storage in plants. Annu Rev Ecol Evol Syst. 21(1):423–447.

Cheong YH, Chang HS, Gupta R, Wang X, Zhu T, Luan S. 2002. Transcriptional profiling reveals novel interactions between wounding, pathogen, abiotic stress, and hormonal responses in Arabidopsis. Plant Physiol. 129(2):661–677.

Cho YW, Park EH, Lim CJ. 2000 Glutathione S-transferase activities of S-type and L-type thiol transferase from *Arabidopsis thaliana*. Biochem Mol Biol j. 33(2):179–183.

Delannoy E, Jalloul A, Assigbetse K, Marmey P, Geiger JP, Lherminier J, Daniel JF, Martinez C, Nicole M. 2003. Activity of class III peroxidases in the defense of cotton to bacterial blight. Mol Plant Microbe Interact. 16(11):1030–1038.

Do HM, Hong JK, Jung HW, Kim SH, Ham JH, Hwang BK. 2003. Expression of peroxidase-like genes, H2O2 production, and peroxidase activity during the hypersensitive response to *Xanthomonas campestris* pv. vesicatoria in *Capsicum annuum*. Mol Plant Microbe Interact. 16(3):196–205.

Edlund AF, Swanson R, Preuss D. 2004. Pollen and stigma structure and function: the role of diversity in pollination. Plant Cell. 16(1):84–97.

Feder N, O'Brien TP. 1968. Plant microtechnique: Some principles and new methods. Am J Bot. 55(1):123–142.

Fisher DB, Jensen WA, Ashton ME. 1968. Histochemical studies of pollen: Storage pockets in the endoplasmic reticulum. Histochemie. 13(2):169-182.

Gomori G. 1950. An improved histochemical technique for acid phosphatase. Stain Technol. 25(2):81–85.

Halliwell B, Gutteridge JM. 1989. 1 Iron toxicity and oxygen radicals. Baillieres Clin Haematol. 2(2), 195–256.

Herrero M, Dickinson HG. 1979. Pollen-pistil incompatibility in *Petunia hybrida*: changes in the pistil following compatible and incompatible intraspecific crosses. J Cell Sci. 36(1):1–18.

Heslop-Harrison Y. 2000. Control gates and micro-ecology: the pollen–stigma interaction in perspective. Ann Bot. 85(1):5–13.

Hiscock SJ, Hoedemaekers K, Friedman WE, Dickinson HG. 2002. The stigma surface and pollen-stigma interactions in *Senecio squalidus* L. (Asteraceae) following cross (compatible) and self (incompatible) pollinations. Int J Plant Sci.163(1):1–16.

Hiscock SJ, Allen AM. 2008. Diverse cell signalling pathways regulate pollen-stigma interactions: the search for consensus. New Phytol. 179(2):286–317.

Hsu RJ, Hsu YC, Chen SP, Fu CL, Yu JC, Chang FW, Chen YH, Liu JM, Ho JY, Yu CP. 2015. The triterpenoids of *Hibiscus syriacus* induce apoptosis and inhibit cell migration in breast cancer cells. BMC Complement Altern Med. 15(1):65–74.

Junglee S, Urban L, Sallanon H, Lopez-Lauri F. 2014. Optimized assay for hydrogen peroxide determination in plant tissue using potassium iodide. Am J Analyt Chem. 5(11):730–736.

Klips RA, Snow AA. 1997. Delayed autonomous self-pollination in *Hibiscus laevis* (Malvaceae). Am J Bot. 84(1):48–53.

Losada JM, Herrero M. 2012. Arabinogalactan-protein secretion is associated with the acquisition of stigmatic receptivity in the apple flower. Ann Bot. 110(3):573–584.

McInnis SM, Desikan R, Hancock JT, Hiscock SJ. 2006. Production of reactive oxygen species and reactive nitrogen species by angiosperm stigmas and pollen: potential signalling crosstalk?. New Phytol. 172(2):221–228.

Neill S, Desikan R, Hancock J. 2002. Hydrogen peroxide signalling. Curr Opin Plant Biol. 5(5):388–395.

Paoletti E, Ferrara AM, Calatayud V, Cervero J, Giannetti F, Sanz MJ, Manning WJ. 2009. Deciduous shrubs for ozone bioindication: *Hibiscus syriacus* as an example. Environ Pollut. 157(3):865–870.

Pearse AG. 1961. Histochemistry, theoretical and applied. Am J Med Sci. 241(1):136.

Punasiya R, Pillai S. 2015. In vitro, antioxidant activity of various leaves extract of *Hibiscus syriacus* L. J Pharmacogn Phytochem. 7(1):18–24.

Quan LJ, Zhang B, Shi WW, Li HY. 2008. Hydrogen peroxide in plants: A versatile molecule of the reactive oxygen species network. J Integr Plant Biol. 50(1):2–18.

Reale L, Sgromo C, Ederli L, Pasqualini S, Orlandi F, Fornaciari M, Ferranti F, Romano B. 2009. Morphological and cytological development and starch accumulation in hermaphrodite and staminate flowers of olive (*Olea europaea* L.). Sex Plant Reprod. 22(3):109–119.

Rodrigo J, Rivas E, Herrero M. 1997. Starch determination in plant tissues using a computerized image analysis system. Physiol Plant. 99(1):105–110.

Rodrigo J, Hormaza JI, Herrero M. 2000. Ovary starch reserves and flower development in apricot (*Prunus armeniaca*). Physiol Plant. 108(1):35–41.

Rodriguez-Garcia MI, M'Rani-Alaoui M, Fernandez MC (2003) Behavior of storage lipids during pollen development and pollen grain germination of olive (*Olea europaea* L.). Protoplasma. 221(3-4):237–244.

Schieber M, Chandel NS. 2014. ROS function in redox signaling and oxidative stress. Curr Biol. 24(10):453–462.

Serrano I, Olmedilla A. 2012. Histochemical location of key enzyme activities involved in receptivity and

self-incompatibility in the olive tree (*Olea europaea* L.). Plant Sci. 197:40–49.
Seymour RS, Blaylock AJ. 2000. Stigma peroxidase activity in association with thermogenesis in *Nelumbo nucifera*. Aquat Bot. 67(2):155–159.
Shakya R, Bhatla SC. 2010. A comparative analysis of the distribution and composition of lipidic constituents and associated enzymes in pollen and stigma of sunflower. Sex Plant Reprod. 23(2):163–172.
Souza EH, Carmello-Guerreiro SM, Souza FVD, Rossi ML, Martinelli AP. 2016. Stigma structure and receptivity in Bromeliaceae. Sci Hort. 203:118–125.
Suarez C, Castro AJ, Rapoport HF, Rodriguez-Garcia MI. 2012. Morphological, histological and ultrastructural changes in the olive pistil during flowering. Sexual Plant Reprod. 25(2):133–146.
Wolters-Arts M, Lush WM, Mariani C. 1998. Lipids are required for directional pollen-tube growth. Nature 392:818–821.
Yanik F, Aytürk Ö, Çetinbaş-Genç A, Vardar F. 2018. Salicylic acid-induced germination, biochemical and developmental alterations in rye (*Secale cereale* L.). Acta Bot Croat. 77(1):45–50.
Zafra A, Rodriguez-Garcia MI, Alche JD. 2010. Cellular localization of ROS and NO in olive reproductive tissues during flower development. BMC Plant Biol. 10(1):36–50.